



The Society shall not be responsible for statements or opinions advanced in papers or discussion at meetings of the Society or of its Divisions or Sections, or printed in its publications. Discussion is printed only if the paper is published in an ASME Journal. Papers are available from ASME for 15 months after the meeting.

Printed in U.S.A.

Copyright © 1993 by ASME

EXPERIMENTAL INVESTIGATION OF THE FLOW IN DIFFUSERS BEHIND AN AXIAL FLOW COMPRESSOR

T. Zierer
Gas Turbine Development
ABB Power Generation Limited
Baden, Switzerland*

ABSTRACT

The flow fields of four diffusers situated at the rear of a one-stage axial flow compressor was experimentally investigated. Through modification of the compressor operating point a wide range of variations of the side wall boundary layers and the radial velocity distribution outside of the boundary layers at diffuser inlet could be achieved. The three dimensional flow field at both diffuser inlet and outlet is analysed. Changes of inlet blockage and radial velocity distribution and their resulting effects on pressure recovery are thoroughly presented. Compared with the results of measurements at diffusers, typically with ducted flow inlet conditions, higher values of pressure recovery are observed. Established design rules, based on investigations of diffusers with carefully developed inlet flow, are checked regarding their applicability for diffusers in turbomachine environment.

NOMENCLATURE

A cross sectional area
 AR area ratio A_2/A_1
 B_1 blocked area at diffuser inlet
 c velocity
 c_p pressure recovery coefficient
 d diameter
 h channel height
 H_{12} $H_{12} = \frac{\delta_{1ax}}{\delta_{2ax}}$
 l approach length before the diffuser
 L averaged wall length for annular diffusers
 \dot{m} mass flow
 Ma Mach number
 p static pressure

P total pressure
 r radius
 Re Reynolds-number
 t pitch
 u axial velocity
 U_∞ velocity at the edge of the boundary layer
 u_t rotor speed at blade tip
 \dot{V} volume flow
 Δx_i distance diffuser inlet/ tip of cone
 y' coordinate in circumferential direction
 y^* coordinate perpendicular to centerline, counting from the wall
 α energy-parameter $\alpha = \frac{1}{A} \int_A \frac{c^2 c_{ax}}{c_{ax}^2} dA$
 β momentum parameter $\beta = \frac{1}{A} \int_A \frac{c^2}{c_{ax}^2} dA$
 $\Delta\gamma$ deviation of the rotor stagger angle from the design point stagger angle
 δ boundary layer thickness
 δ_{1ax} axisymmetric displacement thickness
 δ_{2ax} axisymmetric momentum thickness
 φ Volume flow coefficient $\varphi = \dot{V}/(A \cdot u_t)$
 ζ_D total pressure loss coefficient
 ν kinematic viscosity
 ρ density

Subscripts

ax axial
 i inner
 o outer
 t tip
1 diffuser inlet (control surface I in Fig. 1)
2 diffuser outlet (control surface II in Fig. 1)
3 settling section (control surface III in Fig. 1)

Superscripts

- area averaged
~ mass weighted averaged
' fluctuating quantity

*) The investigation was carried out during the authors previous affiliation at the Thermal Turbomachinery Department, Technische Hochschule Darmstadt, Darmstadt, Germany.

1 INTRODUCTION

Annular diffusers are used in turbomachine environments for a reduction of the velocity at the exit of the bladed duct. Due to the application of a diffuser downstream of a compressor the pressure ratio from flange to flange is increased. A diffuser downstream of a turbine extends the effective enthalpy difference for the bladed part of the machine. A good diffuser design is very important especially for efficiency and performance of one stage machines, because the kinetic energy at the blading exit can be up to 50% of the energy that is transformed by the machine. Nevertheless diffusers for multi-stage machines also require a careful design. Due to the large power of such machines, the kinetic energy at the blading exit can be in the magnitude of several MW.

Up to the present, most investigations of diffusers were carried out without a turbomachine installed upstream of the diffuser. They contributed fundamental knowledge about the design of diffusers and the flow in diffusers at different operating conditions. The most notable contribution concerning annular diffusers is perhaps that due to Sovran and Klomp (1967), who tested more than one hundred annular diffuser geometries with different area and length ratios. All the tests were carried out with ducted flow inlet conditions and a thin inlet boundary layer.

A variation of the inlet conditions was often carried out by changing the inlet blockage B_1 . As a result of their investigations of plane and conical diffusers, Reneau, Johnston and Kline (1967) and Sprenger (1959) concluded, that an increase of inlet blockage leads to a poorer pressure recovery. Another parameter that influences the flow in the diffuser is the swirl at the diffuser inlet. The radial pressure gradient resulting from the swirl leads to poorer turbulent mixing in the hub boundary layer of annular diffusers. Lohmann, Markowski and Brookman (1979) report as a result of their investigation of the swirling flow in annular diffusers, that the onset of flow separation at the diffuser hub occurs earlier than with axial inlet flow. Wolf and Johnston (1969) investigated the influence of non-uniform inlet flow distributions on the pressure recovery in plane diffusers. Inlet profiles with a radial velocity gradient in the core flow resulted in a heavily distorted outlet flow with a larger velocity gradient than at the inlet, due to the deceleration of the flow. Because of this non-uniform velocity distribution at the diffuser exit, the authors obtained a lower pressure recovery than Reneau, Johnston and Kline (1967), who carried out their experiments with plane inlet conditions.

Characteristic for the inlet flow of a diffuser in turbomachine environments is a high level of turbulence and the wakes of the blading situated upstream of the diffuser. Compared to ducted flow inlet conditions, a better pressure recovery may be observed because of the increased turbulent mixing in the diffuser. Both Stevens and Williams (1980) as well as Hoffmann and Gonzales (1984) obtained a considerable increase in pressure recovery compared to ducted flow inlet conditions, when they increased the turbulence level at the diffuser inlet.

Beside investigations showing the basic influence of these parameters, experimental investigations with a real turbomachine situated upstream of the diffuser are also important. Only such experiments show which magnitude those parameters have in the turbomachine and how they influence the flow in the diffuser, when they are superimposed by other parameters such as swirl and velocity distribution at the diffuser inlet.

The present paper is a summary of a detailed investigation of the flow in annular diffusers with inlet conditions typical for an axial flow compressor (Zierer 1992). Due to the wakes of the

compressor blading the inlet flow is characterized by a high level of non-uniformity in the velocity distribution versus radius and versus circumference as well as a high degree of turbulence. As in most of the cases the last row of a compressor is a stator, the inlet flow of the diffuser situated downstream of a compressor is without swirl, independent of the operating conditions.

The measurements were carried out with a one-stage axial flow compressor. They cover a wide operating range of the machine. This results in an wide range of different inlet conditions for the following diffuser. Their impact on the flow in diffusers with different area ratios but constant length shall be discussed. Furthermore, established design rules, based on experimental investigations of diffusers with ducted flow inlet conditions, shall be checked regarding their applicability for diffusers in turbomachine environments.

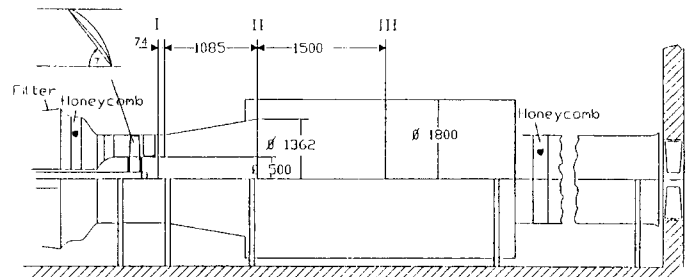


Fig. 1: Test facility with control surfaces I, II, III

2 EXPERIMENTAL APPARATUS

Fig. 1 shows a cross-section of the test rig. The air is drawn from the laboratory through a nozzle to the compressor blading. The annular diffuser is mounted behind the stage. The diffuser walls are hydraulically smooth. Behind the diffuser the flow expands into a settling section followed by a tube where the mass flow can be determined.

The compressor stage is designed for constant work versus radius. The design volume flow coefficient is $\varphi = 0.335$. The blading profiles are based on the NACA 65 series according to a design procedure of Lieblein (1965). The solidity of the stator ranges from 2.4 at the hub to 1.1 at the tip (25 vanes). The ratio of compressor hub to tip is 0.5. The flow in the rotor has been thoroughly investigated by Sieber (1986).

During the measurements, the volume flow in the system was varied at constant 2000rpm by adjusting a throttle device at the exit of the facility. A desired volume flow coefficient could be regulated within 1%. The investigations were carried out at design stagger angle of the rotor blading $\Delta\gamma = 0^\circ$ as well as at a smaller stagger angle $\Delta\gamma = -8^\circ$, respectively. The stagger angle of the stator was kept constant throughout all measurements. Due to the sufficient solidity of the stator blading, the swirl at the exit of the stage did not exceed $\pm 5^\circ$. At maximum mass flow ($\Delta\gamma = 0^\circ$) the mean velocity at the stator exit amounted to 40m/sec. The corresponding Reynolds number $Re = \frac{c_1 \cdot h_1}{\nu}$ is $6.6 \cdot 10^5$, the Mach number $Ma = 0.1$.

All measurements were carried out with pneumatic probes (5 hole probes and pitot probes). Both at diffuser inlet and diffuser outlet probe traverses were carried out versus radius and circumference. The static pressure distribution along the diffuser was measured with static pressure taps at hub and casing.

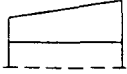

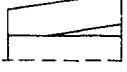
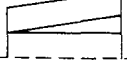
	d_{1i} [mm]	d_{1o} [mm]	d_{2i} [mm]	d_{2o} [mm]	Δz_1 [mm]	l_{ax} [mm]	$\frac{L}{h_1}$ [-]	AR [-]
	500	1000	500	1362	-	1085	4.36	2.14
	500	1000	627	1362	713	1085	4.37	1.95
	500	1000	738	1362	389	1085	4.39	1.75
	500	1000	855	1362	40	1085	4.40	1.50

Table 1: Tested diffuser geometries

Probe positioning as well as data recording was performed by a microcomputer. Depending on the measuring position, the signals have different fluctuations versus time. To obtain a representative mean value, a sufficient number of samples was taken, from which a mean value was calculated. The required number of samples was determined during the measurements for each measurement position. The confidence interval achieved, resulting from the standard deviation of the fluctuations and the number of samples taken, ensures that the difference between the real mean value and the mean value averaged from the samples is less than 0.4% of the measuring range with a statistic security of 95%. The resulting statistic security of velocity and pressure recovery is $c/\bar{c} = 1.5\%$ (diffuser inlet), $c/\bar{c} = 5.5\%$ (diffuser outlet) and $c_p = 4.5\%$. This was solely not reached at total pressure measurements in separated flow regions.

The diffuser geometries which were tested are listed in Table 1. At a constant length ratio $L/h_1 = 4.4$ the area ratio AR ranges from 1.5 to 2.14. The total area ratio from diffuser inlet to the settling section amounts $A_3/A_1 = 4.4$. The diffuser with $AR = 1.95$ is designed for maximum pressure recovery at a prescribed length according to the design criteria of Sovran and Klomp. It is located on the c_p^* line in the diffuser performance map of the authors. Therefore, even at healthy inlet conditions in the larger diffuser with $AR = 2.14$ a flow separation at the diffuser exit must be expected. The remaining two diffusers are designed more conservatively. At the same length ratio they have lower area ratios.

The investigations of Sovran and Klomp showed that the influence of the wall shape is small compared to the influence of the main dimensions, area ratio and length ratio. Investigations of plane diffusers by Carlson et al. (1967) showed that a slightly increase in c_p could be reached for diffusers situated below the c_p^* line when the side walls had a bell shape. Considering these results, the reduction of the area ratio at constant length ratio was incorporated by moving a cone at the diffuser hub towards the diffuser inlet. The cone was divided in three axial parts, so that casing and hub of the diffuser always ended at the same axial position. The resulting geometries all lead to a favourable increase rate of cross section area versus diffuser length, because the diffusion rate is reduced at the end of the diffuser where the boundary layers are thick. Therefore, it was expected that a difference in pressure recovery at a fixed operation point is predominantly caused by a different area ratio and not by the different wall shapes.

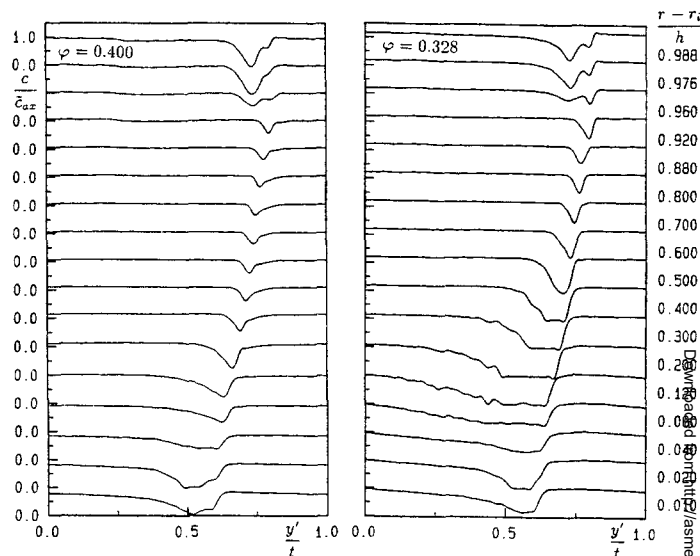


Fig. 2: Comparison of the flow field at diffuser inlet at different volume flow coefficients ($AR = 2.14, \Delta\gamma = 0^\circ$)

3 VELOCITY DISTRIBUTIONS

Due to the streamline curvature at the diffuser inlet, the static pressure in this plane is not constant. Preparatory Measurements with a five-hole probe showed that the static pressure distribution versus radius could be well approximated by a linear interpolation between three measurement points (hub, half-channel height and casing). Therefore, all velocity distributions and the performance coefficients ζ and c_p were evaluated with a static pressure distribution interpolated from the three measuring points mentioned above.

Fig. 2 shows the velocity distribution behind a stator blade. Probe traverses were carried out behind three different stator blades. Thereby, good circumferential symmetry was observed. The largest wakes occur at the hub. Here the flow separates at the suction side at small volume flow coefficients φ due to the increased loading of the blading.

For almost the same operation points the velocity distribution at diffuser exit is shown in Fig. 3. In this plane, a good circumferential symmetry was observed as well. At small volume flow coefficients a separated region at the hub can be seen. Only in this zone the flow is not axisymmetric. In fact, the flow here was

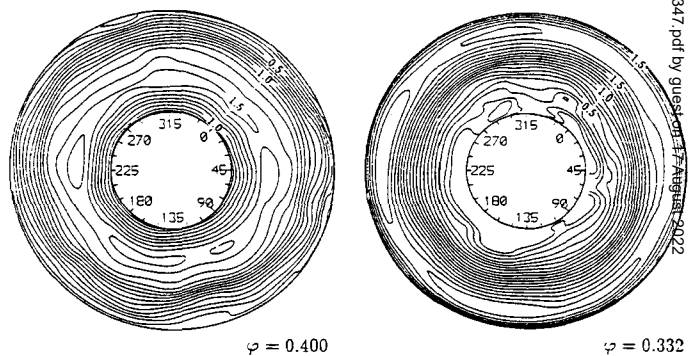


Fig. 3: Contour lines of constant velocity $\frac{c}{c_{ax}}$ at diffuser exit ($AR = 2.14, \Delta\gamma = 0^\circ$)

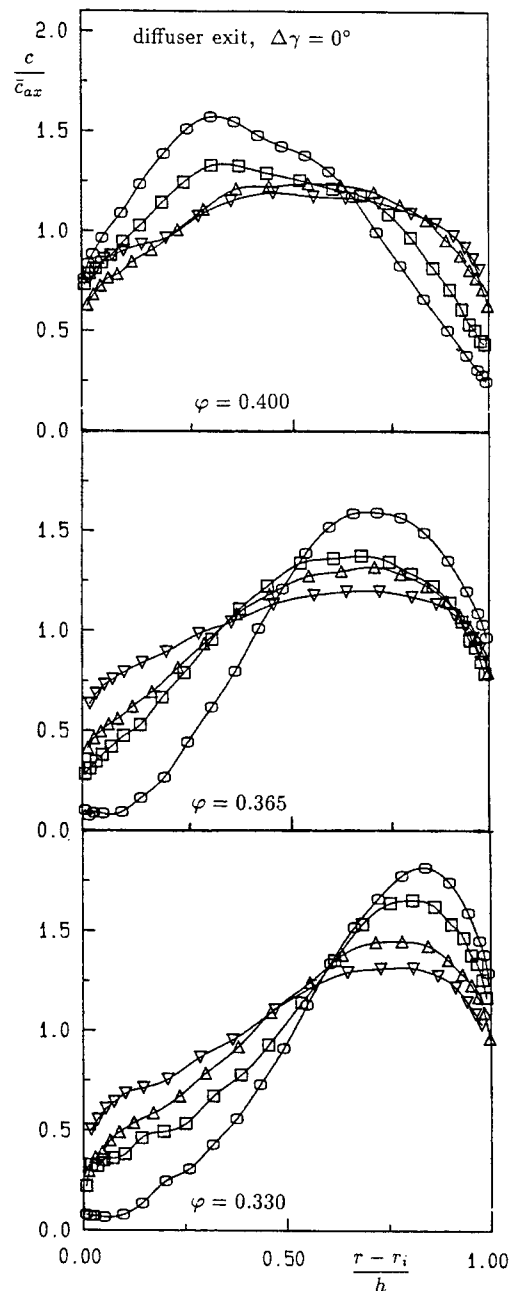
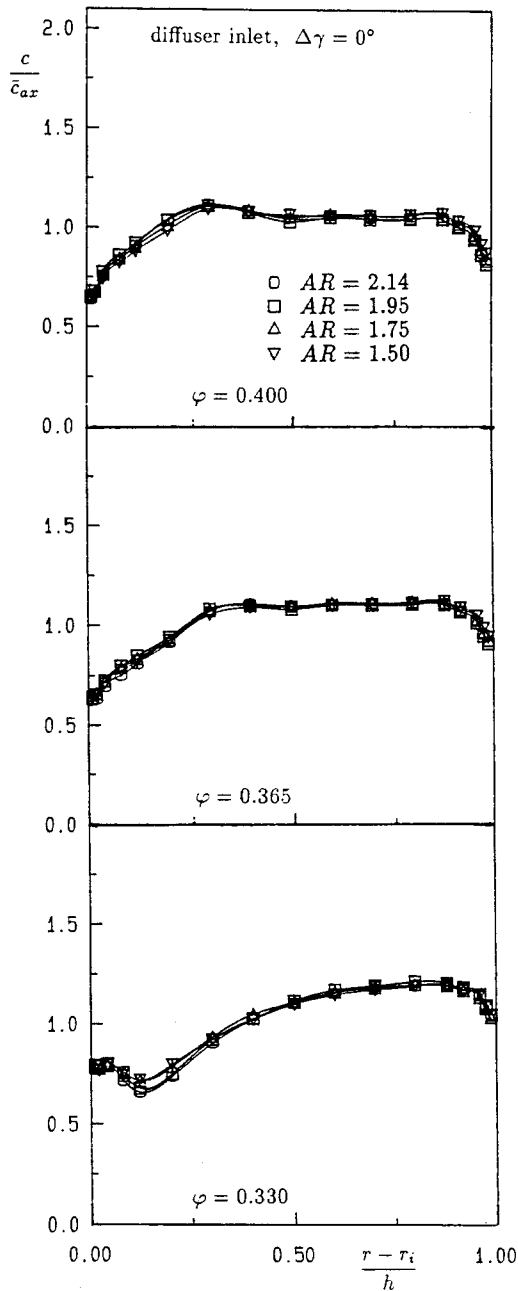


Fig. 4: Dependence of the velocity profiles at diffuser exit on the pitch averaged inlet profile and the area ratio ($\Delta\gamma = 0^\circ$)

very unsteady, so that the time-averaged mean values could not be evaluated with the statistical security mentioned above. Furthermore, the velocity gradient in this zone is very small. Both effects contribute to comparatively large deflections of the contour lines of constant velocity in the separated zone.

In Fig. 4 and 5 the circumferentially area-averaged velocity distributions at diffuser inlet are compared with their corresponding velocity distributions at the diffuser outlet. At the design point stagger angle the inlet velocity profiles are characterized by a constant velocity in the core flow. When the mass flow is reduced, the hub sidewall boundary layer increases strongly.

The inlet velocity distributions at smaller stagger angle ($\Delta\gamma = -8^\circ$) differ from the profiles at design point stagger

angle. Here the core flow is characterized by a radial velocity gradient combined with a high energetic maximum near the hub. As in the case $\Delta\gamma = 0^\circ$ the boundary layer at the hub increases when the volume flow is reduced.

The velocity distributions of the hub and casing boundary layer at both diffuser inlet and diffuser outlet were compared with the two dimensional velocity model of Pfeil and Mueller (1989). For turbulent flows, this model is an extension of Cole's Model. Except for the cases with strong separation at the stator blading (i. e. $\Delta\gamma = 0^\circ$, small φ) a good agreement with the model was observed. Therefore, the circumferentially-averaged flow field in the diffuser may be considered as two dimensional, if stage loading is not too high.

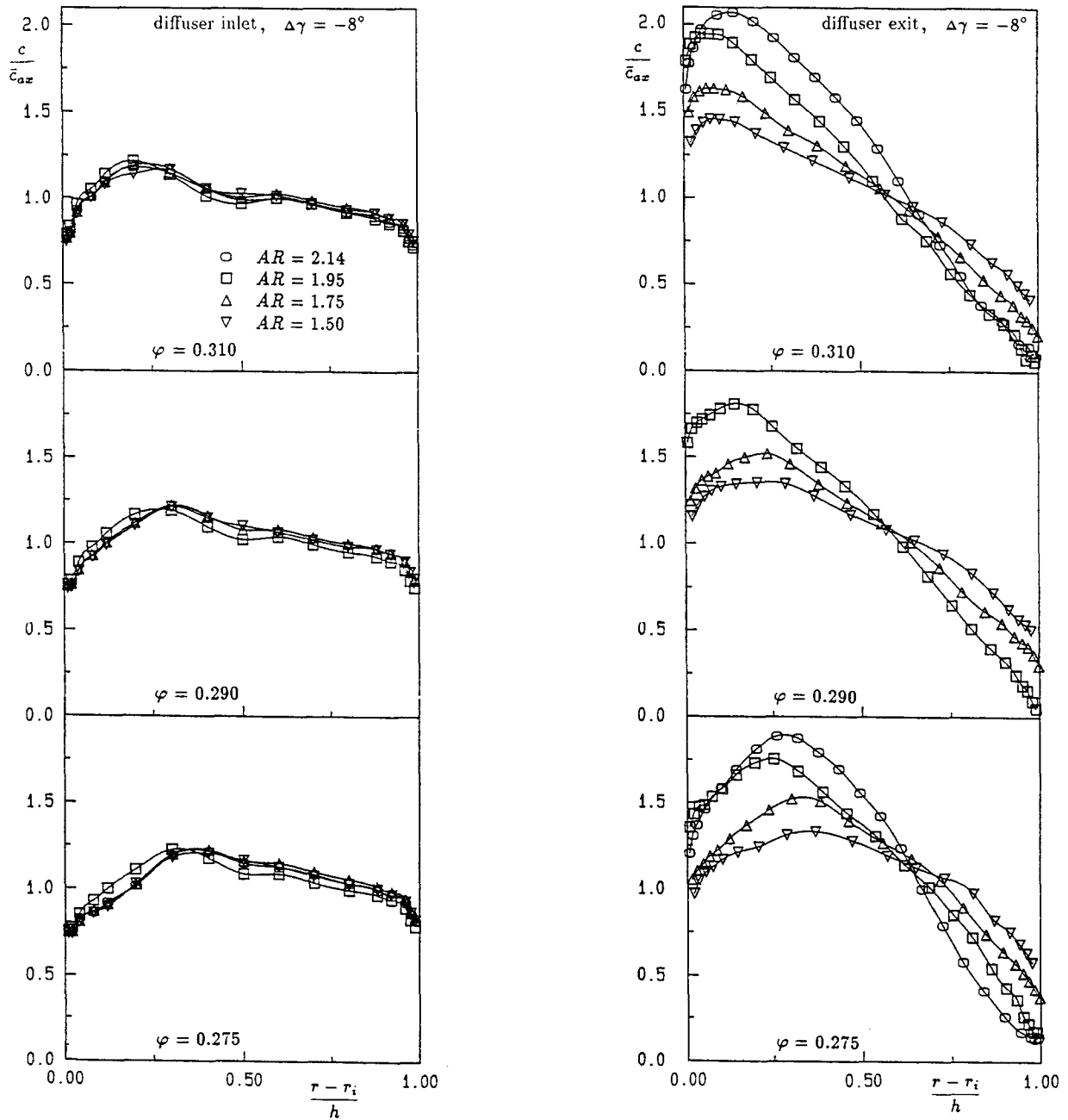


Fig. 5: Dependence of the velocity profiles at diffuser exit on the pitch averaged inlet profile and the area ratio ($\Delta\gamma = -8^\circ$)

In Fig. 6 and 7 the axisymmetric displacement thickness δ_{1ax} and the shape parameter H_{12} are plotted.

$$\delta_{1axi} = \int_0^\delta \left(1 - \frac{u}{U_\infty}\right) \left(1 + \frac{y^*}{r_i}\right) dy^* \quad (1)$$

For the casing wall r_i must be replaced by $-r_o$. Due to the non uniformity of the core flow the distinction between the boundary layer and the core flow is difficult. Therefore, the boundary layer thickness δ resulting from the velocity model was taken as upper integration boundary and displacement thickness calculated by integration of the measured distribution up to this boundary.

At constant stagger angle the loading of the blading increases with decreasing volume flow coefficient. This results in a strong growth of the displacement thickness at the hub at the diffuser inlet. Nevertheless, the shape parameter remains almost constant and at low values. At the casing the flow is nearly independent of the loading.

Focusing on the results with constant velocity versus radius of the inlet coreflow (i.e. $\Delta\gamma = 0^\circ$), it can be seen that increasing displacement thickness leads to flow separation along the diffuser at the hub. As expected, the separation occurs earlier (i.e. at a larger volume flow coefficient) when the area ratio is increased. As mentioned above, in contrast to the displacement thickness

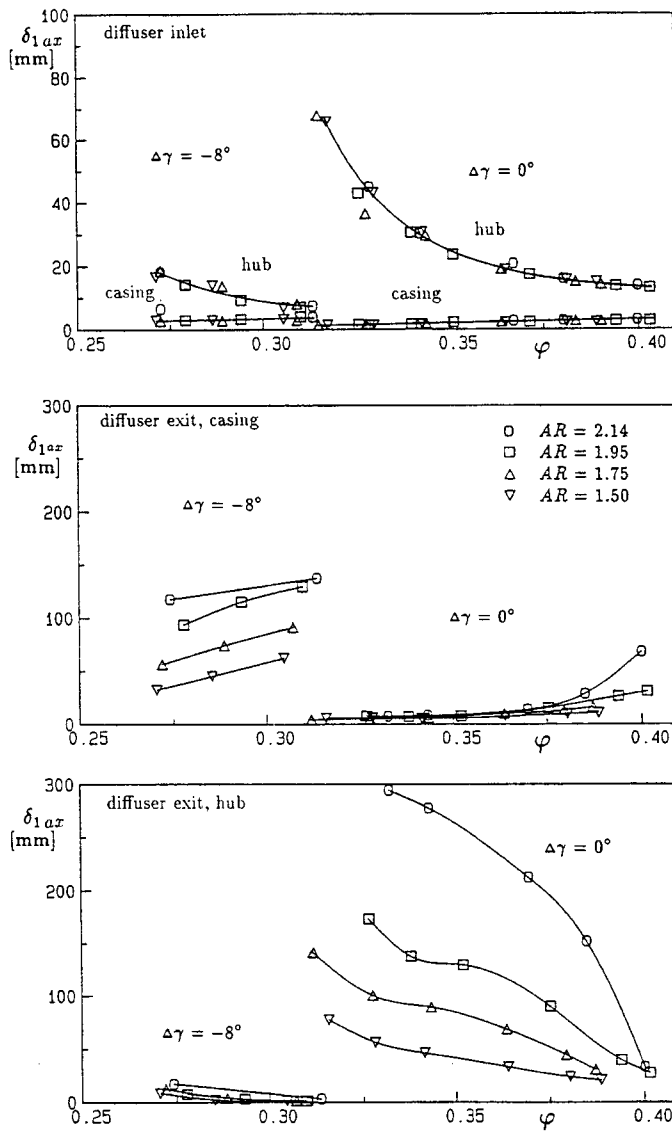


Fig. 6: Displacement thickness δ_{1ax} at both diffuser inlet and diffuser exit

the shape parameter at the diffuser inlet remains nearly constant throughout all operating points. Therefore, it can be concluded from the present experiments that the shape parameter is not the quantity which determines the behaviour of the flow in a diffuser downstream of a compressor when the operation point is changed. While the displacement thickness of the sidewall boundary layer increases with the stage loading the shape parameter remains nearly constant. Therefore, the displacement thickness is the determining boundary layer parameter. Moreover, as a result of their numerical investigation of the flow in conical diffusers Schlichting and Gersten (1961) state that the growth of the boundary layer along a diffuser depends only weakly on the shape parameter at the diffuser inlet. They established the momentum thickness as the determining quantity. The results of this paper also indicate that the thickness of the boundary layer is an important parameter for the flow downstream in the diffuser. Because the shape parameter did not vary in the course of the experiments, no con-

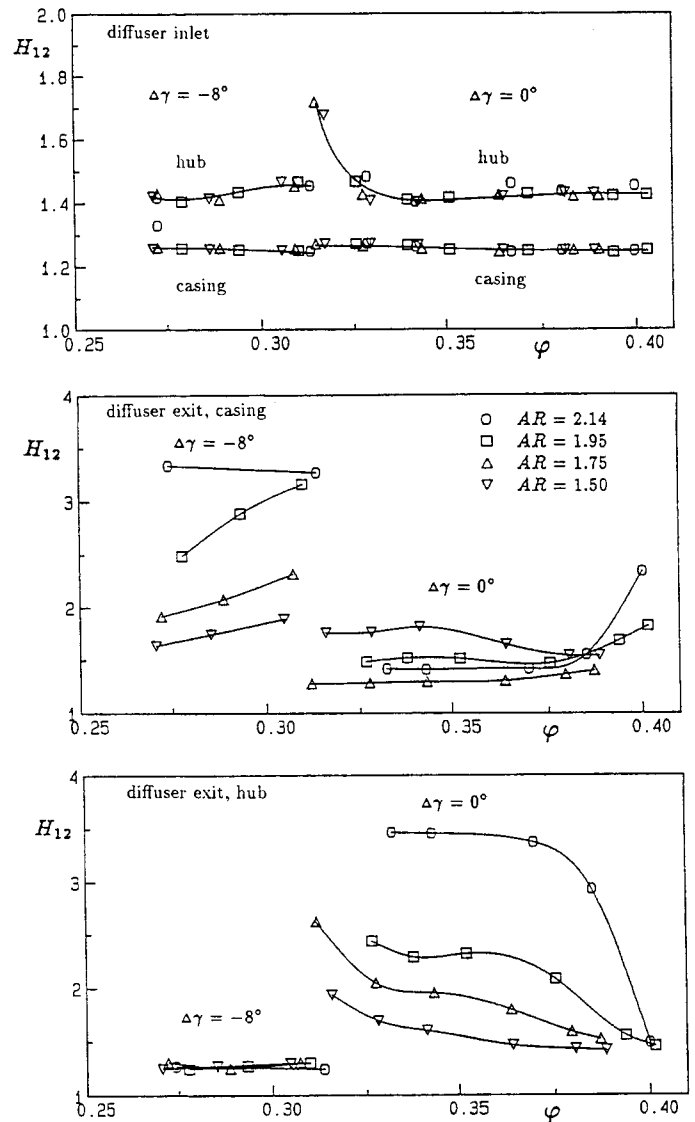


Fig. 7: Shape parameter H_{12} at both diffuser inlet and diffuser exit

clusions can be made here as to whether displacement thickness or momentum thickness do have the determining influence.

Besides the influence of the inlet boundary layer on the flow in the diffuser, there is also a strong influence of the radial velocity distribution outside the boundary layers. This is shown by a comparison of the measurements at different stagger angles. At the design point stagger angle of the rotor ($\Delta\gamma = 0^\circ$), the velocity distribution versus radius remains almost constant in the core flow for all volume flow rates. Here, the flow separates along the hub of the diffuser as the hub boundary layer at the diffuser inlet increases. In the case $\Delta\gamma = -8^\circ$ the inlet velocity is characterized by a radial velocity gradient combined with a high energetic maximum at the hub. Although the inlet boundary layers are almost the same as in the case $\Delta\gamma = 0^\circ$, i.e. the hub boundary layer is much thicker than the casing boundary layer, a separation at the diffuser casing occurs here. The resulting non-uniformity at the diffuser exit is much bigger than at hub separation.

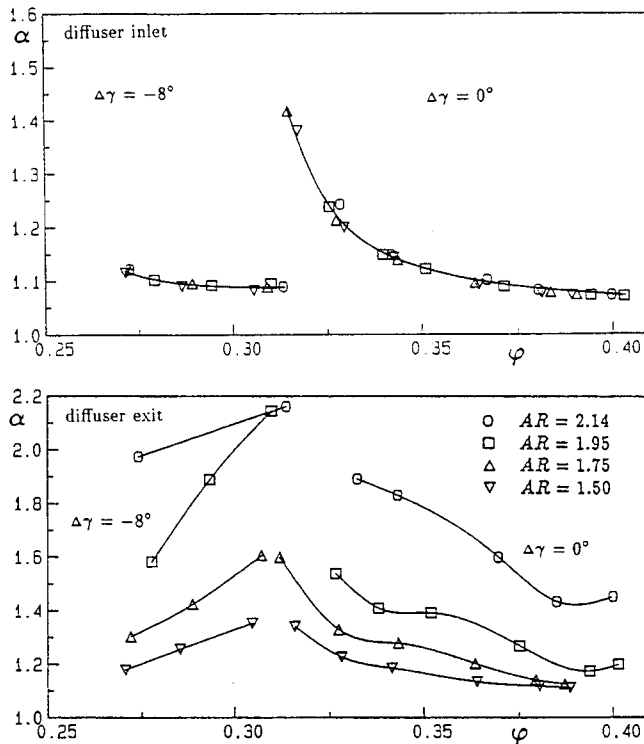


Fig. 8: Energy parameter α at both diffuser inlet and diffuser outlet

In sum it may be said that small changes of the inlet profile do have large influence on the flow in the diffuser, especially when the area ratio of the diffuser is large at a small length ratio. Thereby, axisymmetric separation at one sidewall leads to a more stable flow pattern at the opposite wall.

The boundary layer parameters δ_1 and H_{12} describe the circumferentially averaged velocity profiles at one wall. An integral quantity, describing the velocity distribution in an entire cross section is the energy coefficient α . To give a measure of the magnitude of the flow non-uniformity the energy coefficient is plotted in figure 8. At the diffuser inlet it is determined half from the radial velocity distribution and half from the wakes of the blading, respectively. At the diffuser exit, the portion due to circumferential non-symmetry, is negligible. This shows that at turbomachinery inlet conditions the energy coefficient is considerably higher compared to ducted flow inlet conditions. For example, Stevens (1980) reports energy coefficients between 1.02 and 1.06, depending on the approach length of the annular duct upstream of the diffuser.

4 PERFORMANCE EVALUATION

From the previous section it may be concluded that the radial velocity distribution and the displacement thickness are the most important inlet flow parameters influencing the flow in the diffuser when the operating point of the compressor is altered. In this section, the impact on pressure recovery of varying these parameters shall be discussed in more detail.

For a one dimensional description of the diffuser flow, the total pressure loss coefficient and the pressure recovery coefficient are applied. These are defined by

$$\zeta = \frac{2\Delta\bar{P}}{\rho \alpha_1 \bar{c}_{1ax}^2} \quad (2)$$

and

$$c_p = \frac{2(\bar{p}_2 - \bar{p}_1)}{\rho \alpha_1 \bar{c}_{1ax}^2} \quad (3)$$

The energy parameter α is defined by the energy equation and describes the additional kinetic energy the flow contains due to its radial and circumferential non-uniformity compared to a flow with a plug profile.

$$\bar{p}_1 + \frac{\rho}{2} \alpha_1 \bar{c}_{1ax}^2 = \bar{p}_2 + \frac{\rho}{2} \alpha_2 \bar{c}_{2ax}^2 + \Delta\bar{P} \quad (4)$$

The analysis of the measurements showed that the difference between the area-weighted and mass-weighted mean value of the static pressure was negligible. To simplify evaluation procedure the area-weighted mean value was applied for the calculation both the pressure recovery coefficient and the total pressure loss coefficient.

For the one dimensional description of the influence of both, hub and casing boundary layer the blocked area (Sovran and Klomp, (1967) or Klein, (1981)) is applied

$$B_1 = \frac{2\pi(r_{1i}\delta_{1axi} + r_{1o}\delta_{1axo})}{\pi(r_{1o}^2 - r_{1i}^2)} \quad (5)$$

When the operating point of the compressor is altered several parameters influencing pressure recovery in the diffuser are changing. Therefore, the pressure recovery coefficient c_p is plotted in Fig. 9. versus the volume flow coefficient φ . Obviously the volume flow coefficient is not a determining parameter for the flow in the diffuser. It is only used for a distinction of the different inlet conditions resulting from the different operating points.

In the control plane diffuser exit at the design stagger angle ($\Delta\gamma = 0^\circ$) the maximum pressure recovery is obtained at an area ratio of 1.95, almost independent of the operating point. Here, over all operating points the change of the flow field at the diffuser inlet is dominated by the change in the inlet blockage. The independence of the optimum area ratio on the inlet blockage is in close agreement with Sovran and Klomp's analysis (1967) of the flow in conical and plane diffusers having ducted flow inlet conditions. They report only a negligible change in the c_p^* line when the blockage at the diffuser inlet was increased, implying that the optimum area ratio, leading to maximum pressure recovery at constant length ratio, is independent of the inlet blockage. This also applies to diffusers in turbomachine environments. Moreover, the diffuser with the area ratio 1.95 agrees very well with the c_p^* line in the diffuser performance map by Sovran and Klomp. This demonstrates that the results of their systematic investigation are often a good tool for designing diffusers in turbomachine environments, even though the data were derived from ducted flow inlet conditions. Nevertheless the use of these correlations should be restricted to inlet conditions which resemble those used by Sovran and Klomp. Typically, for a turbomachine situated upstream of a diffuser the increased inlet turbulence and the wakes present a slightly improvement of these inlet conditions, leading to a higher pressure recovery yet no change in the optimum area ratio. This is no longer true for heavily distorted inlet flows, as the measurements at $\Delta\gamma = -8^\circ$ show. Compared to the increasing blockage, the particular radial velocity gradient imposed on the core flow at the experiments represents a much worse distortion of the inlet flow. Therefore, the maximum pressure recovery is obtained at smaller area ratios.

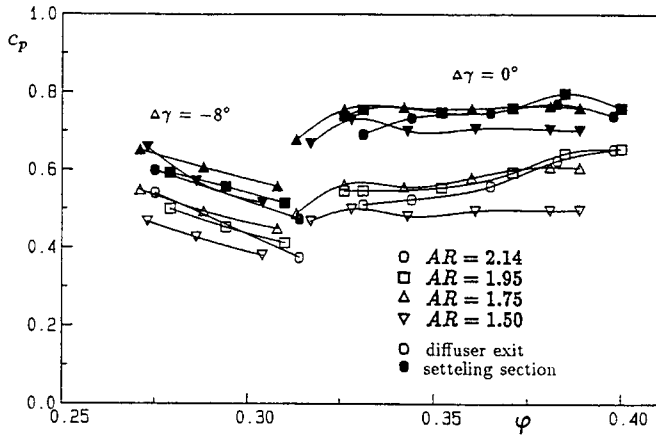


Fig. 9: Dependence of pressure recovery c_p on area ratio and operation point of the compressor

In the settling section a considerable increase of the pressure recovery is observed. This indicates the importance of such a device behind a diffuser. The additional pressure recovery is caused by both an increase of the area ratio and an equalisation of the velocity profile. From the momentum equation

$$\Delta c_p = 2 \left(\frac{A_1}{A_3} \right)^2 \left(\beta_2 \frac{A_3}{A_2} - \beta_3 \right) \quad (6)$$

with

$$\beta = \int_A \frac{c^2}{\bar{c}_{ax}^2} dA \quad (7)$$

it can be concluded that a high pressure recovery is obtained both by means of large area ratios $\frac{A_3}{A_2}$ and by a high non-uniformity of the flow field at the diffuser exit resulting in large momentum parameters β_2 . Therefore, the differences concerning c_p , resulting from different inlet conditions or diffuser area ratios, become smaller in the settling section. At constant area ratios, a decrease in c_p in plane II due to a distorted inlet flow results in a larger non-uniformity of the velocity at diffuser exit increasing the pressure recovery in the settling section. By analogy, poor pressure recovery due to a small diffuser area ratio A_2/A_1 is also compensated by an increased pressure recovery in the settling section because of the increased area ratio A_3/A_2 .

The examination of the velocity plots shows that the displacement thickness is an important quantity which influences the flow in the diffuser if the radial velocity distribution at the inlet remains constant. Fig. 10 shows the dependence of the pressure recovery coefficient on inlet blockage and area ratio. With increasing blockage a poorer pressure recovery is obtained. When the area ratio is increased, a growing influence of the inlet blockage on pressure recovery can be established: Here a change of blockage especially at small values of B_1 is accompanied by a rapid decrease of c_p . From the velocity plots it can be seen that in this particular case the change of the inlet blockage is accompanied by the onset of separation at the diffuser hub.

Obviously, compared to the influence of the inlet blockage, a change in the radial velocity distribution outside the boundary layer has a more pronounced effect on pressure recovery. The operating points at $\Delta\gamma = -8^\circ$ are characterized by a radial velocity gradient in the inlet core flow, leading to a high energetic ma-

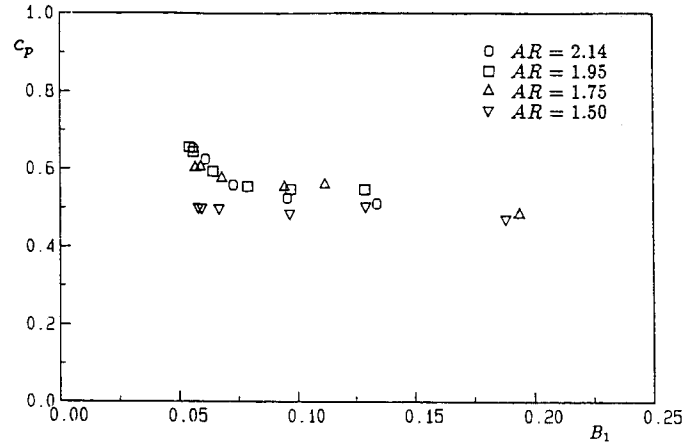


Fig. 10: Dependence of pressure recovery c_p at diffuser exit on inlet blockage B_1 (constant velocity versus radius in the inlet core flow)

ximum near the hub. The displacement thickness is of the same magnitude as at $\Delta\gamma = 0^\circ$ and large volume flow coefficients, however there the velocity versus radius in the core flow at the diffuser inlet is constant. At $\Delta\gamma = -8^\circ$ the particular radial velocity gradient at the experiments combined with the bend at the casing causes a separation at the casing leading to a considerable lower pressure recovery. The flow has to overcome a higher pressure rise at the diffuser casing than at the diffuser hub due to the convex turning, whereby the inlet flow has the lowest energy level at the casing resulting from the radial velocity distribution. Here, at $\Delta\gamma = -8^\circ$ even a rise in pressure recovery can be observed with increasing blockage which increases with decreasing volume flow coefficient. Thus the improved pressure recovery is caused by the equalisation of the inlet core flow at lower volume flow coefficients.

	$AR = 1.5$	$AR = 1.95$
$\varphi = 0.38 (\Delta\gamma = 0^\circ)$	5%	8%
$\varphi = 0.33 (\Delta\gamma = 0^\circ)$	5%	13%
$\varphi = 0.30 (\Delta\gamma = -8^\circ)$	6%	8%
$\varphi = 0.28 (\Delta\gamma = -8^\circ)$	6%	12%

Table 2: Typical values of total pressure loss $\zeta_{12} = \frac{2(\bar{P}_1 - \bar{P}_2)}{\rho \alpha_1 \bar{c}_{1ax}^2}$

Table 2 lists typical values of total pressure loss. Beside the diffuser loss depending on area ratio and radial velocity distribution at the diffuser inlet, this total pressure drop also contains the loss due to the decay of the wakes of the compressor. The lowest total pressure losses are achieved at small area ratios due to the weak deceleration of the flow. Stevens and Wray (1985) report losses between 14% and 18% in a pre-combustor diffuser behind a one-stage axial flow compressor.

From the energy equation the relation

$$c_p = 1 - \frac{\alpha_2 \bar{c}_2^2}{\alpha_1 \bar{c}_1^2} - \zeta_{12} \quad (8)$$

can be derived. This shows, that poor pressure recovery is caused by total pressure losses and poor velocity deceleration. Depending on operating conditions and area ratio the total pressure loss amo-

Author	AR	L/h ₁	Re = $\frac{\rho h_1 u}{\mu}$	B ₁	c _p	inlet conditions
Stevens/Williams	2.0	5.0	0.55 · 10 ⁵	0.028	0.505	annular duct, approach length l/h ₁ = 7.3
Stevens/Williams	2.0	5.0	0.55 · 10 ⁵	0.109	0.445	annular duct, approach length l/h ₁ = 44.0
Stevens/Williams	2.0	5.0	0.55 · 10 ⁵	0.044	0.595	annular duct, approach length l/h ₁ = 7.3 with coarse grid for turbulence increasement
Quest/Scholz	2.05	4.0	2.0 · 10 ⁵		0.71	diffuser behind turbine
Adenubi	2.0	4.5	6.0 · 10 ⁵	0.085	0.58*	diffuser behind compressor
Zierer	1.95	4.4	6.5 · 10 ⁵	0.056	0.67	diffuser behind compressor (φ = 0.40)
Zierer	1.95	4.4	4.5 · 10 ⁵	0.054	0.56*	diffuser behind compressor (φ = 0.28) radial velocity gradient

Table 3: Comparison of several experimental diffuser investigations *) $c_p = \frac{p_2 - p_1}{\rho/2c_1^2}$

unts to 5% – 14% of the dynamic pressure at the diffuser inlet. Therefore, the total pressure loss as a fraction of the difference between the maximum obtainable pressure recovery and the measured value only amounts to

$$\frac{\zeta_{12}}{1 - c_p} = 0.1 \dots 0.3. \quad (9)$$

The larger portion is caused by an insufficient diffusion. At large area ratios the reason for insufficient diffusion is a non-uniform velocity distribution at the diffuser exit. At smaller area ratios the energy parameter at the diffuser exit decreases, but this decrease is accompanied by a corresponding increase of the area-averaged velocity \bar{c}_2 .

A comparison of the pressure recovery obtained at the diffuser exit with the results from other authors shows that in diffusers situated downstream of a turbomachine a higher c_p value is obtained. Table 3 lists the results of several experimental investigations of diffusers with nearly identical geometries. Stevens (1980) reports a c_p value of 0.5 for ducted flow inlet conditions. Comparable, regarding the inlet blockage, are the measurements at high volume flow coefficient at $\Delta\gamma = 0^\circ$ where a c_p value of 0.67 is obtained. Compared to the present investigations, Quest and Scholz (1981) report a considerably higher pressure recovery in a diffuser situated downstream of a one-stage axial turbine. This may be caused by smaller sidewall boundary layers and the leakage flow at the casing. The mean values of the state variables are calculated using an averaging procedure by Kreitmeier (1992) which takes into account all balance equations and is characterized by hypothetical reversible and irreversible equilibration processes. For incompressible flow without swirl the reversible mean values are close to the mean values used in this paper. The pressure recovery measured by Adenubi in a compressor diffuser is considerably smaller. Moreover, he relates the pressure rise to the dynamic pressure calculated from the area-averaged mean value of the velocity, which leads to larger c_p values. The poor pressure recovery may be explained by the inlet conditions, which were characterized by a radial velocity gradient with a maximum near the hub as in the case $\Delta\gamma = -8^\circ$ in the present investigations. The c_p value of this operating point calculated with the area-averaged mean value of the velocity is of the same magnitude as in Adenubi's investigations.

The higher pressure recovery in turbomachine environments is due to the increased turbulence at the diffuser inlet. The compressor used upstream of the diffusers investigated in this paper is the same as that described by Goeing (1987). He reported an axial degree of turbulence

$$Tu = \frac{\sqrt{u'^2}}{\bar{u}} = 7\%$$

outside of the stator wakes and outside of the sidewall boundary layers. The averaged value must be considerably higher. A part of this turbulence is due to the periodic oscillations, induced by the rotor, but Adenubi (1976) reports from his measurements behind a one-stage axial flow compressor, that the rotor induced periodic oscillations amount to only 1%. He reports area-averaged axial stochastic turbulence intensities between 5% and 7%. Also, Stevens observed an increase in c_p after he increased the turbulence level at the diffuser inlet with application of a coarse grid in front of the diffuser. The increased turbulence produces a better momentum transport perpendicular to the main flow direction. This results in a later onset of separation and a higher pressure recovery.

5 CONCLUSIONS

The flow fields in four diffusers with inlet conditions typical for an axial flow compressor were experimentally investigated. Characteristic for the diffuser inlet flow in turbomachine environments are the wakes of the blading upstream of the diffuser and a high degree of turbulence. The operating point of the compressor situated before the diffusers was varied in a wide range. As a result of these investigations it was found that of the parameters changing with the operating point of the compressor, those having the most influence on the flow in the diffuser were the displacement thickness and the radial velocity distribution in the core flow at the diffuser inlet.

For a wide operating range of the compressor, when the change of the inlet conditions is dominated by a variation of the inlet blockage but velocity versus radius remains constant in the core flow, design rules for annular diffusers based on ducted-flow inlet conditions may also be applied for diffuser design in turbomachine environments.

Compared with diffusers, typically with ducted-flow inlet conditions, diffusers in turbomachine environments achieve a considerably higher pressure recovery. This is due to the increased turbulent mixing resulting in a later onset of separation.

In addition to inlet blockage influence the flow in the diffuser is strongly influenced by the radial velocity distribution in the core flow at the diffuser inlet. The particular radial velocity gradient imposed during the experiments combined with the bend at the casing caused a considerably lower pressure recovery than in the case of constant velocity.

Regarding the influence of the radial velocity distribution, a potential for increasing turbomachine efficiency is inherent, when the diffuser and the turbomachine are well matched to one another. During the design of the blading special attention should be taken of the exit velocity profile which can be easily calculated using through flow codes. Further information about the influence of the radial inlet velocity distribution on the flow in diffusers is still sought. There is no doubt that the optimum inlet distribution will depend on the meridional shape of the diffuser, as the flow direction often must be turned in diffusers due to design limitations very strongly. This is an area where further investigations about the influence of the inlet conditions on the flow in diffusers should be pursued.

DEDICATION

This paper is dedicated to Prof. Dr.-Ing. H. Pfeil, who initiated and greatly supported this work, but died before the preparation of this manuscript.

REFERENCES

- Adenubi, S.O. (1976), Performance and Flow Regime of Annular Diffusers With Axial Turbomachine Discharge Inlet Conditions. *Journal of Fluids Engineering* Vol. 98, pp. 236-243.
- Carlson, J.J., Johnston, J.P., Sagi, C.J. (1967), Effects of Wall Shape on Flow Regimes and Performance in Straight, Two-Dimensional Diffusers. *Journal of Basic Engineering* Vol. 89, pp. 151-160.
- Hoffmann, J.A., Gonzales, G. (1984) Effects of Small-Scale, High Intensity Inlet Turbulence on Flow in a Two-Dimensional Diffuser. *Journal of Fluids Engineering* Vol. 106, pp. 121-124.
- Johnson, I.A., Bullock, R.O. (1965), Aerodynamic Design of Axial-Flow Compressors. National Aeronautics and Space Administration, Washington D.C..
- Klein, A. (1981), Review: Effects of Inlet Conditions on Conical-Diffuser Performance. *Journal of Fluids Engineering* Vol. 103, pp. 250-257.
- Kreitmeier, Franz (1992), Space-Averaging 3D Flows Using Strictly Formulated Balance Equations in Turbomachinery, Paper published at the ASME Cogen 1992.
- Lohmann, R.P., Markowski, S.J., Brookman, E.T. (1979), Swirling Flow Through Annular Diffusers With Conical Walls. *Journal of Fluids Engineering* Vol. 101 pp. 224-229.
- Pfeil, H., Sieber, J. (1986), Characteristic Factors of a Compressor Rotor in Comparison With Two-Dimensional Cascade Data. ASME Paper 86-GT-29.
- Pfeil, H., Sieber, J. (1986), Velocity Distribution and Decay Characteristics of Wakes Behind a Compressor Rotor-Blade. ASME Paper 86-GT-115.
- Pfeil, H., Göing, M. (1987) Measurements of the Turbulent Boundary Layer in the Diffuser Behind an Axial Flow Compressor. *Journal of Turbomachinery* Vol. 109, pp. 405-412.
- Pfeil, H., Müller, T. (1989), Velocity Profile Modell for Two-Dimensional Zero-Pressure Gradient Transitional Boundary Layers. *AIAA Journal*, Vol. 27, pp. 1127-1132.
- Quest, J., Scholz, N. (1981), Experimentelle Untersuchungen von Nabendifusoren hinter Turbinenstufen. Abschlußbericht zum FVV-Vorhaben Nr. 4468 Nabendifusoren, DFVLR, Institut für Antriebstechnik, Köln.
- Reneau, L.R., Johnston, J.P., Kline, S.J. (1967), Performance and Design of Straight, Two-Dimensional Diffusers. *Journal of Basic Engineering* Vol. 89 pp. 141-150.
- Schlichting, H., Gersten, K. (1961), Berechnung der Strömung in rotationssymmetrischen Diffusoren mit Hilfe der Grenzschichttheorie. *Zeitung für Flugwissenschaften* Bd. 9, pp. 135-140.
- Sovran, G., Klomp, E.D. (1967), Experimentally Determined Optimum Geometries for Rectilinear Diffusers with Rectangular, Conical or Annular Cross-Section. *Fluid Mechanics of Internal Flow*, Elsevier Publishing Company, Amsterdam, London, New York.
- Sprenger, H. (1959), Experimentelle Untersuchungen an geraden und gekrümmten Diffusoren. Dissertation, ETH Zürich.
- Stevens, S.J., Nayak, U.S.L., Preston, J.F., Robinson, P.J., Scrivener, C.T.J. (1980), The Influence of Compressor Exit Conditions on the Performance of Combustor Dump Diffusers. *Journal of Aircraft*, Vol.15, No.8 pp. 482-488.
- Stevens, S.J., Williams, G. (1980), The Influence of Inlet Conditions on the Performance of Annular Diffusers. *Journal of Fluids Engineering* Vol. 102, pp. 357-363.
- Stevens, S.J., Wray, A.P. (1985), The Influence of Blade Wakes on the Performance of Outwardly Curved Combustor Pre-Diffusers AIAA paper 85-1291.
- Wolf, S., Johnston, J.P. (1969), Effects of Nonuniform Inlet Velocity Profiles on Flow Regimes and Performance in Two-Dimensional Diffusers. *Journal of Basic Engineering* Vol. 91 , pp. 462-474.
- Zierer, Th. (1992), Experimentelle Untersuchung der Strömung in Diffusoren mit verschiedenen Erweiterungsverhältnissen hinter einem Axialverdichter. Doctoral Thesis, TH Darmstadt, Darmstadt, Germany.